A Proposal of an RF Fingerprint-based Outdoor Localization Technique using Irregular Grid Maps

Gustavo P. Bittencourt, Anderson A. F. Urbano and Daniel C. Cunha
Centro de Informática (CIn)
Universidade Federal de Pernambuco (UFPE)
Recife-PE, Brazil
{gpb3, aafu, dcunha}@cin.ufpe.br

***Abstract*—Location techniques have an increasing demand nowadays. As opposed to the global positioning system (GPS), radio frequency (RF) fingerprint-based techniques are low-energy solutions with reasonable precision and easy implementation. In general, it works by dividing a location area into a grid map and defining an RF pattern to each grid cell in an attempt to uniquely identify it. The most common grid layout is the square grid model (i.e., regular grid) where all cells are equally spaced. In this paper, we propose an RF fingerprint-based location method using an irregular grid layout whose shape resembles the road network of an urban region. The proposed model aims to diminish computational complexity while maintaining or even improving the location estimation precision.**

***Index Terms*—location system, outdoor positioning, fingerprinting, irregular grid, received signal strength**

I. Introduction

Locating mobile users with increasing accuracy in a wireless communication environment is one of the major challenges of recent positioning systems [1]. Techniques based on the global positioning system (GPS) have been widely chosen as a reasonable solution for such a problem. Although very popular, GPS-based techniques are often inefficient when applied indoor or in dense urban environments. The accuracy degradation mainly occurs due to multipath propagation in weak signal conditions typically caused by buildings blockage [2]. In addition, it is well-known that GPS-based techniques are highly energy hungry. This characteristic can pose a problem, for example, in context-aware applications deployed on top of wireless sensor network (WSN) devices, where recharging batteries could not be feasible. To extend their lifetime, these devices should opt for energy saving strategies [3], [4].

Over the past few years, fingerprint-based techniques have emerged as an alternative capable of locating mobile users in both indoor and outdoor environments. Radio Frequency (RF) fingerprint-based techniques are capable of locating mobile users with an accuracy of tens of meters [9], which comply with the FCC's E911 requirements for wireless services. Such precision can be sustained even in non-line-of-sight (NLOS) environments [6]. The performance in NLOS conditions makes RF fingerprint-based localization techniques suitable for application in dense urban environments. Moreover, these techniques are built to leverage cellular infrastructure support, offering a good trade-off between the location estimation precision and the deployment cost.

The overall purpose of RF fingerprint-based techniques is to split the coverage region (location area) into small subregions by means of a square grid. The coverage region represents the area in which mobile devices will be moving around. The main goal is to obtain a signal level indication for each grid cell concerning a set of base stations (BSes) which position and transmitted power are previously known. This information is used to build what we call a radio map of the coverage region.

The key concept of the radio map relies on the fact that signal fluctuations are distinct between grid cells and can be used to uniquely identify each one. Since the geographic position of each grid cell is known, it is possible to determine the location of a mobile device by comparing its signal level in an unknown position with the ones stored in the radio map. The radio map measurement, which correlates in a high degree with the signal level obtained by the mobile device, could potentially provide a good estimation of the mobile real position. Previous works related to RF fingerprint-based techniques focus mainly on the application of machine learning (ML) algorithms to improve the radio map building and the correlation phase [5], [7], [8]. The majority of grid-based location approaches uses square grid maps (i.e, regular grids) in order to represent the coverage area. However, there are few investigations targeting the impact of grid geometry in the location estimation precision [9], [10].

Based on that, we propose an approach to improve both precision and performance by using irregular grid maps in RF fingerprint-based location applied to dense urban environments. The proposed grid model is capable of fitting to the urban road network. Such property drastically reduces the number of cells in the grid map which impacts on both performance and location estimation precision. The proposed grid model exploits the fact that in dense urban environments, like metropolitan downtown areas which are massively occupied by residential and commercial buildings, outdoor mobile users will most probably be moving through the urban road network or in places nearby such as sidewalks and footbridges. This assumption makes reasonable to choose grid layouts that are well-fitted for such areas. Furthermore, specialized applications like the ones targeting user mobility could take

advantage of these grid layout strategies. The results obtained show that the proposed irregular grid layout resulted in a 69.7% reduction in the number of grid cells on average while slightly improving the location precision in about 4 meters in all simulations performed.

The outline of the paper is organized as follows. Section II briefly discusses related work. Section III describes irregular grid maps and details how the experiments were performed. In Section IV, the obtained results are presented by performing a comparison between the different grid models. Finally, in Section V, conclusions and future investigations are drawn.

II. Related Work

Kim, Min and Yeo [9] proposed an algorithm based on a statistical significance test to determine if two geographically close RF-fingerprints can be clustered together. The average distance between RF-fingerprints in neighbor clusters is used to calculate the area of each grid cell. Such algorithm when applied to a database of RF-fingerprints entails in an irregular grid segmentation. Although the result appears promising, the authors stated that some improvements on the estimation precision are, in part, due to the increase in the number of grid cells promoted by the segmentation process: as a side effect the clustering algorithm generates extra grid cells when compared to the reference grid used throughout the analysis. Despite that fact, the ratio between the location estimation precision improvement and the number of extra grid cells added due to the clustering algorithm is positive. The location estimation improvement ranged from 25.7% to 30.1% while the average grid cell increment was 11.2%.

Han, Ma and Zhang [10] proposed an irregular grid model in which the area of the grid cells are defined based on its distance to the base station (BS) following a radial geometry. The key concept behind the proposed segmentation is that the signal quality is better in the surroundings of the BS than far away. The region nearby the BS is less subject to signal fluctuations, therefore, a larger value for the grid cell area is assigned to such region. On the other hand, the signal power is expected to drop at a certain distance from the BS, affecting the received signal strength more severely even when considering small distance changes. For such regions a small value is assigned to the area of each grid cell. The evaluated grid models take into account two and three levels with different grid cell areas in each one. The results were obtained through simulations and shown an improvement up to 16% in the location estimation precision when compared to the regular grid model.

III. Proposed Approach

The general architecture of fingerprint-based location systems consist of offline and online phases. The overall purpose of the offline phase is to generate a feature vector which can be used to uniquely identify each cell in the grid map. The grid cell position is typically defined as a GPS coordinate and the feature vector is composed by signal properties that can be measured or predicted concerning that specific GPS coordinate. As an example, the received signal strength (RSS) related to a set of BSes can be taken as a feature vector where each feature is an RSS value. Following, an RSS-feature vector must be assigned to each cell in the grid map, ultimately generating what is called a radio map.

The RSS-feature vector is commonly obtained in a non-automatic way, typically by performing a drive-test across the coverage region. Considering the non-automatic nature of the driving-test, it becomes impractical to obtain the RSS-feature vector for all grid cells in the coverage region. As a side-effect, some grid cells' RSS values cannot be collected, therefore, the RSS-feature vector is not assigned.

An usual solution for this problem is to employ a regression algorithm to assign values to the grid positions where the RSS values are unknown. The regression algorithm takes the GPS coordinates associated to each grid cell as an input and works by providing a predicted RSS value for a particular BS at that point in space. For the purpose of this research, we decided to use a variation of the K nearest neighbors (KNN) algorithm called weighted KNN (W-KNN). KNN is an instance-based algorithm that takes a validation sample as input and chooses the K closest samples in the training set (i.e., nearest neighbors) by using some metric function such as the Euclidean distance. At last, the chosen K samples are averaged to predict the output sample [11]. Based on that, the W-KNN algorithm uses a parameter W to weight the importance of each neighbor. The weight values are obtained by measuring the distance between the K nearest neighbors and the validation sample. Finally, all K weights are taken into account when calculating the output sample. The W-KNN algorithm was chosen since its implementation is relatively simple when compared to other ML algorithms such as artificial neural network (ANN), support vector machine (SVM) or random forest. Also, the W-KNN algorithm has been applied as a reasonable solution in localization problems [12], [13]. In the context of this work, the output of the W-KNN algorithm, denoted as $RSS_{i,c}$, is the predicted RSS value for the i-th BS at the cell c of the grid map and is given by

$$RSS_{i,c} = \frac{\sum_{j=1}^{K} RSS_{i,j} \left(\frac{1}{d_{c,j}}\right)^{W}}{\sum_{j=1}^{K} \left(\frac{1}{d_{c,j}}\right)^{W}}, \tag{1}$$

where K is the number of neighbors, $RSS_{i,j}$ is the RSS value for the i-th BS at the j-th neighbor, $d_{c,j}$ is the geodesic distance between the GPS coordinates of the cell c and the j-th neighbor. At the end, W determines the importance of that distance in the final output. If $W = 0$, all distances will have equal weight in the output and thus, the algorithm becomes equivalent to the KNN regressor.

After the radio map generation, the online phase can take place when a new sample needs to have its location determined. To do that, a matching operation that selects the most similar cell of the radio map is performed. The position of the mobile user is then given by the location of the cell

center. Different similarity functions can be used to accomplish the matching operation, but Euclidean distance is the most common metric.

The process of constructing a regular grid model is straightforward. Based on the boundaries established by the coverage region, by means of its GPS coordinates, it is possible to split that region into smaller square cells. To control the number of cells in the final grid map, the side of each square cell (in meters), here named as *resolution*, can be provided as an input to the regular-grid generation algorithm. A higher resolution implies in an increase of the number of grid cells, since the distance between two consecutive grid cell centers decreases and, consequently, the square cell area.

In contrast to the regular grid model, the process for constructing the irregular grid maps are divided into two steps. Fig. 1 illustrates the workflow for the generation of irregular grid maps. The first step, illustrated by Fig. 1(a), is executed only once and focuses on the acquisition of a map skeleton formed by several street segments that can be used to represent the road network in the coverage area. For this, we used the OpenStreetMap (OSM) Project, which is an open-license community-driven effort to maintain a high quality map database for general purpose usage [14]. Using this tool, we download a map database corresponding to our coverage region. Since the file adheres to the OSM XML file format specification, we parse its contents to retrieve all the GPS coordinates associated to each street found inside the coverage region. Such coordinates are stored as street segments which are used later to build the grid maps. After that, the second step, depicted by Fig. 1(b), concentrates on the grid map generation by using the street segments obtained in the first step. As defined for the regular grid, we use the resolution as an input parameter to control the number of cells in the final grid map. However, in the irregular-grid context, resolution is defined as the distance (in meters) between the coordinates of two adjacent cells. The main purpose of this step is to use the distance established by the resolution to interpolate every two adjacent coordinates contained in each street segment. The generation process finishes by merging all interpolated street segments into a greater set named grid map.

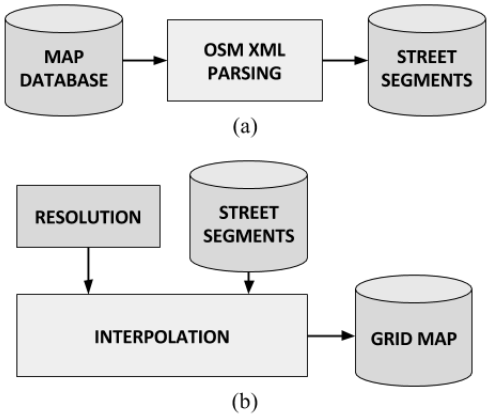

Figure 1. Diagram of the irregular grid generation process: (a) Obtaining the street segments (first step). (b) Grid map generation (second step).

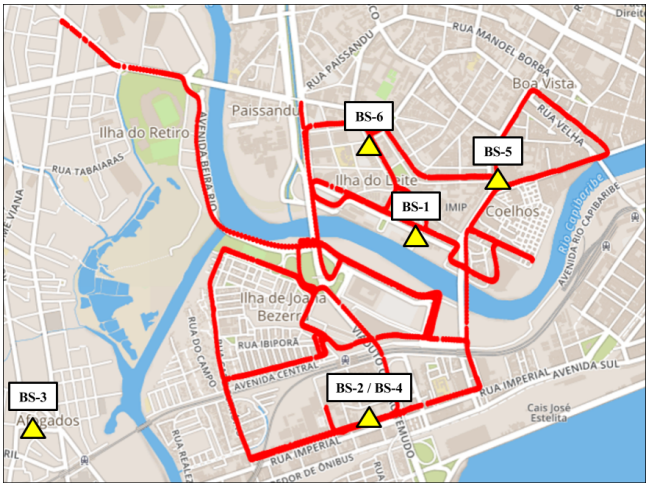

Figure 2. Urban environment of the city of Recife-PE, Brazil. The position of the base stations (triangles) are indicated as well as the collected measurements (marked line).

To demonstrate how the irregular grid generation process works, consider the urban environment of the city of Recife-PE, Brazil, illustrated in Fig. 2, where $2,756$ measurements were taken to compose the map database. The drive-testing route used to build the dataset is indicated by the marked line. These measurements were collected for cellular Global Mobile System Communication (GSM) technology at the 1.8 GHz RF spectrum. This is an extended version of the dataset used by Timoteo et al. in [7]. The original dataset used in [7] covers an area of approximately two square kilometers with measurements from three BSes, while, in this study, we use data obtained from six BSes. Each measurement in the dataset contains an RSS value in dB units, measured for all six BSes, at known GPS coordinates. The yellow triangles in Fig. 2 indicate the location of the BSes. It is important to highlight that both BS-2 and BS-4 are located in the same place, i.e., their GPS coordinates match. Nonetheless, their antennas cover different regions, where each one is specialized in best-serving a different region.

Based on the location area, we built 40 grid maps, whereas

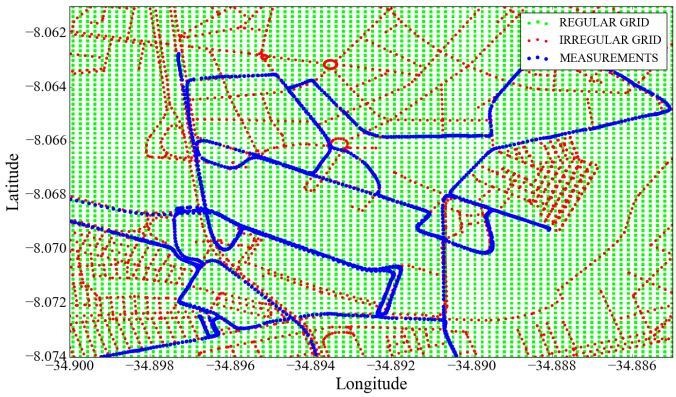

Figure 3. Partial measurement database and generated grids for targeted location area: 20 m-resolution regular and irregular grid.

20 of them had square-grid geometry (regular) and the remaining 20 followed the urban road network geometry (irregular). In our experiment, the resolution is considered a value in the interval $[1 - 20\,\text{m}]$, with one meter per step. Fig. 3 shows part of the measurement database and illustrates the difference between a regular grid and our street-based irregular grid. Both grids use a 20m resolution parameter and each cell is represented by its center coordinates.

Table I presents the grid maps created for our experiment. For a given resolution, we have the number of cells for the grid type. Concerning the number of cells, the 11 m-resolution irregular grid is equivalent to the 20 m-resolution regular grid in order of magnitude. Indeed, it is important to emphasize that this cell-amount equivalence tends to repeat itself between both grid models when we consider other resolution values. For example, take the 3 m-resolution irregular grid and the 11 m-resolution regular grid.

It is well-known that the location estimation error tends to decrease when resolution gets higher. On the other hand, the computational cost fastly grows for high resolutions in a way that using such values can be prohibitive for practical scenarios. In addition, there is a trade-off between resolution and location estimation precision. In some cases, it is not worth to increase the resolution in detriment of the computational cost [15]. A benefit from using irregular grid maps relates to the fact that low cell growth rates make it possible to experiment higher resolution values without penalizing the computational cost.

The radio map generated using W-KNN regressor follows the same geometry defined for the grid map except that, in the radio map, the RSS-feature vector related to the known BSes are computed for all grid cells. The RSS values are calculated for each BS by using a W-KNN regressor with fixed parameters $K = 3$ and $W = 1$. Such parameter combination improved the location estimation precision in our experiment.

In addition to the RSS-feature vector, the timing advance parameter value is appended to each radio map cell. This parameter, denoted by TA, is represented by an integer greater than zero ($TA \geq 1$) and can be obtained from the GSM protocol through a specific control channel. The parameter TA can be interpreted as a quantized value, in steps of 550 m, which represents the distance between the mobile user and the BS. For example, $TA = 1$ indicates that the mobile is located within 550 m radius from the BS; when $TA = 2$, the mobile is located in a distance between 550 m and 1110 m from the BS and so forth [16].

The purpose of the TA parameter is to act as a filter to reduce the search space at the validation phase. Typically, reducing the search space implies decreasing the computational cost in checking every validation sample against each cell in the radio map. This characteristic tends to improve the performance by minimizing the location system response time. The Algorithm 1 gives the pseudo-code of how the filtering process is implemented in our experiment. In this algorithm, B represents the set of BSes, R is the radio map, s is the validation sample and $TA(s, b)$ is the TA value for sample s with respect to the b-th BS. The function $CellSubset(b, taValue)$ selects the set of all cells with certain TA value for the b-th BS and R' corresponds to the reduced set obtained by TA-filtering of the original radio map R.

Algorithm 1 TA filter for search space reduction

```
1: function TAFILTER(B, R, s)
2:     R' ← R                          ▷ The filtered grid starts full
3:     for b ∈ B do
4:         taValue ← TA(s, b)
5:         bsSubset ← CellSubset(b, taValue)
6:         R' ← R' ∩ bsSubset
7:     if R' == ∅ then
8:         R' ← R
9:     return R'
```

Fig. 4 gives an overview of the RF fingerprint-based localization technique proposed in this work. Firstly, we have the radio map generation process illustrated in Fig. 4(a), where the grid map coordinates are taken jointly with the collected RSS measurements to generate a radio map (offline phase). As explained in Section IV, the RSS samples are obtained by taking the drive-testing measurements as partitioned by each k-fold iteration. Moreover, the process should be aware of the coordinates from all BSes. Afterward, a validation sample is checked against the radio map database (online phase). This process, shown in Fig. 4(b), is conducted by first applying the TA filter to reduce the search space and later by using a similarity function to choose the GPS coordinates that better match the validation RSS fingerprint given as input.

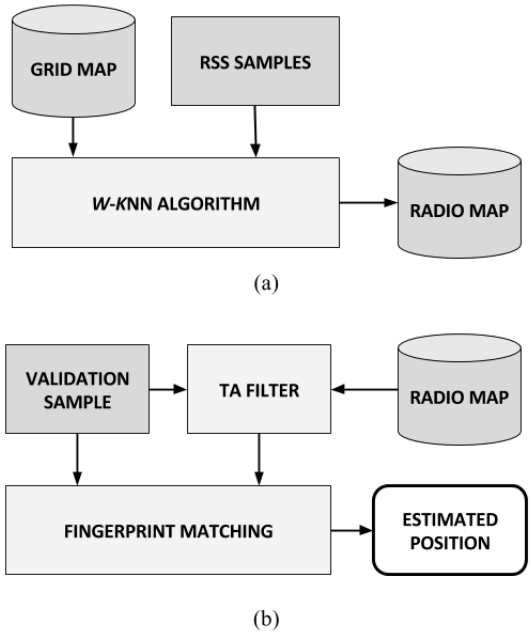

Figure 4. Diagram of the RF fingerprint-based localization technique: (a) Fingerprint training process (radio map generation). (b) Fingerprint matching process (location prediction).

Table I
NUMBER OF CELLS GENERATED FOR THE GRID MAPS UNDER DIFFERENT RESOLUTIONS.

Resolution	**Regular** (cells)	**Irregular** (cells)	**Resolution**	**Regular** (cells)	**Irregular** (cells)
1 m	4,231,360	99,631	11 m	35,055	10,453
2 m	1,058,224	50,718	12 m	29,516	9,951
3 m	470,492	34,421	13 m	25,230	9,329
4 m	264,792	26,282	14 m	21,574	8,805
5 m	169,273	21,370	15 m	18,875	8,365
6 m	117,750	18,094	16 m	16,638	7,945
7 m	86,349	15,784	17 m	14,763	7,585
8 m	66,316	14,031	18 m	13,104	7,274
9 m	52,250	12,622	19 m	11,781	7,025
10 m	42,300	11,622	20 m	10,622	6,557

IV. NUMERICAL RESULTS

The performance of the proposed RF fingerprint-based localization technique, considering regular and irregular grids, is evaluated by computer simulations. To estimate the accuracy of our proposal, we use a statistical method called k-fold cross-validation, a re-sampling method that randomly divides the samples into k subsets (named as folds) of approximately equal size [17]. These folds are organized in two categories: the validation set with only one fold and the training set with $(k-1)$ folds. At each iteration, $(k-1)$ folds are selected for training the model (i.e., generating the radio map - see Fig. 4(a)), while one fold is reserved for validation (block "Validation Sample" in Fig. 4(b)).

In this paper, we consider $k = 10$ and use the average grid-location error μ and its standard deviation σ_μ as cross-validation metrics to evaluate the performance of both regular-grid and irregular-grid layouts. The average grid-location error μ is defined as

$$\mu = \frac{1}{k}\sum_{j=1}^{k} e_j \ , \tag{2}$$

where e_j is the average error calculated for the j-th validation fold, that is given by

$$e_j = \frac{1}{T}\sum_{s=1}^{T} e_{j,s} \ , \tag{3}$$

where $e_{j,s}$ corresponds to the location estimation error associated with sample s that belongs to the j-th validation fold, and T is the number of samples in the j-th validation fold. The error $e_{j,s}$ is defined as

$$e_{j,s} = |\mathbf{p} - \mathbf{p}_s| \ , \tag{4}$$

where $\mathbf{p}$ is the predicted position while $\mathbf{p}_s$ is the real position associated with the validation sample. The difference between $\mathbf{p}$ and $\mathbf{p}_s$ is taken by measuring the geodesic distance from $\mathbf{p}$ to $\mathbf{p}_s$. It is important to highlight that $\mathbf{p}_s$ is previously known, once it is collected as part of the drive-test measurements and is solely used to calculate $e_{j,s}$.

Fig. 5 shows the behavior of the average grid-location error μ in respect to the grid resolution. The standard deviation σ_μ ranges from 1.5 to 2.5 m interval. We can see that, for all grid resolutions considered in this study, irregular-grid layouts are more accurate than regular-grid ones when predicting locations. The results show that, in our RF fingerprint-based proposal, irregular-grid layouts improve the location precision around 3.85 m on average. In addition, Fig. 5 reveals that for higher resolution values, the difference between the obtained average grid-location error μ for regular and irregular grids increases. For the 20 m-resolution, the error is 58 m for the regular grid and 52 m for the irregular one, which implies in a difference of 6 m. However, the overall improvement tends to decay for higher resolution values. For example, considering the grid map resolutions equal to or less than 13 m, the error difference ranges from 3 to 4 m.

Overall, we can state that the irregular grid model performs better for all grid map resolutions regarding the average grid-location error μ. However, the results show an improvement of only a few meters. Considering the fact that the proposed irregular-grid models are supposed to be used in an outdoor environment, the error improvement by itself might not be sufficient to justify the adoption of irregular-grid layouts. The main difference between both grid models is more remarkable when we consider the number of cells required to reach a specified error requirement. For example, to achieve an aver-

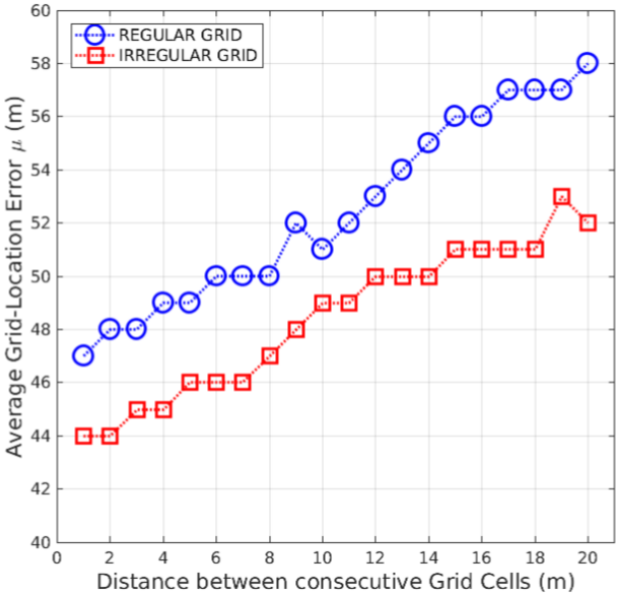

Figure 5. Average grid-location error μ versus the distance between two consecutive grid cells for both regular-grid and irregular-grid layouts.

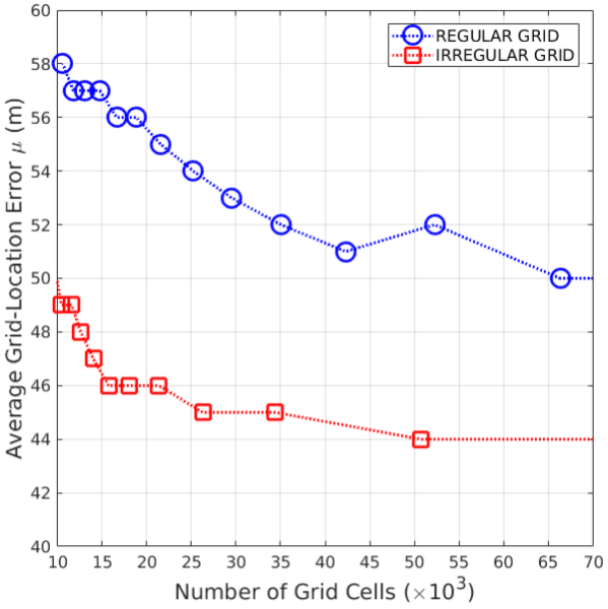

Figure 6. Average grid-location error μ versus number of grid cells for both regular-grid and irregular-grid layouts.

age grid-location error of 51 m or less, we can take the 18 m-resolution irregular grid. In order to reach the same location error, a regular grid of at least 10 m-resolution must be used. Observing Table I, the 18 m-resolution irregular grid has $7,274$ cells, whereas the 10 m-resolution regular grid has $42,300$ cells. The number of cells in the regular grid is approximately six times greater if compared to the quantity of cells in the irregular one. This characteristic makes the irregular grid feasible to use higher resolution values to improve the location estimation precision without drastically increasing the number of cells.

An important aspect that deserves attention regards the fact that the number of cells in the grid maps is a major concern since it directly affects the performance of practical location systems by increasing the computational cost. The usage of higher resolution values for the regular-grid models become prohibitive for real applications given the increasing cell growth rate. In contrast, irregular-grid layouts allow us to increase the location precision without penalizing the location system response time and computational cost.

As shown in Table I, by comparing the number of cells, it is possible to assert that the 9 m-resolution regular grid is equivalent to the 2 m-resolution irregular grid. As illustrated in Fig. 6, by taking the $52,250$-cells regular-grid (9 m-resolution) and the $50,718$-cells irregular-grid (2 m-resolution), the error difference between both grid models is equal to 8 m. Such improvement seems reasonable to bring a positive impact in the location estimation position. Lastly, when focusing on location precision, we suggest that both grid models are compared concerning the number of cells, not the resolution.

V. Conclusions

In this work, we proposed an RF fingerprint-based localization approach using irregular grid maps for outdoor environments. The proposed grid model was capable of fitting to urban road network. Numerical results showed that an irregular grid, that follows the road network in an urban region, was more accurate for RF fingerprint-based positioning than a regular square grid. In addition, the proposed irregular grid proved to be efficient in terms of computational complexity. In other words, for the same region, the number of cells generated in the irregular grid was smaller than the number in regular ones, even in a case of higher resolutions. Finally, it is meaningful to emphasize that the proposed localization approach can be applied to most recent generations of cellular networks as 3G, 4G, and so on. For future work, we intend to apply an analytical framework, such as stochastic geometry, to investigate the theoretical performance of the model.

Acknowledgment

This work was supported by Tempest Security Intelligence, a global cyber security company with presence in Brazil and in the UK, as well as the research cooperation project between Motorola Mobility (a Lenovo Company) and CIn-UFPE.

References

[1] R. Rahdar, J. T. Stracener and E. V. Olinick, "A systems engineering approach to improving the accuracy of mobile station location estimation," *IEEE Syst. J.*, v. 8, n. 1, pp. 14–22, 2014.

[2] J. Soubielle, I. Fijalkow, P. Duvaut and A. Bibaut, "GPS positioning in a multipath environment," *IEEE Trans. Signal Processing*, v. 50, n. 1, pp. 141–150, 2002.

[3] A. M. Abu-Mahfouz and G. P. Hancke, "ALWadHA localization algorithm: yet more energy efficient," *IEEE Access*, v. 5, pp. 6661–6667, 2017.

[4] S. K. Rout, A. K. Rath and C. Bhagabati, "Energy efficient dynamic node localization technique in wireless sensor networks," *Indian J Sci Technol*, v. 10, n. 15, pp. 1–8, 2017.

[5] Q. D. Vo and P. De, "A survey of fingerprint-based outdoor localization," *IEEE Commun. Surv. Tuts.*, v. 18, n. 1, pp. 491–506, 2016.

[6] I. Guvenc and C. -C. Chong, "A survey on TOA based wireless localization and NLOS mitigation techniques," *IEEE Commun. Surv. Tuts.*, v. 11, n. 3, pp. 107–124, 3rd Quart. 2009.

[7] R. D. A. Timoteo, L. N. Silva, D. C. Cunha, G. D. C. Cavalcanti, "An approach using support vector regression for mobile location in cellular networks," *Computer Networks*, v. 95, pp. 51–61, 2016.

[8] H. Liu, H. Darabi, P. Banerjee and J. Liu, "Survey of wireless indoor positioning techniques and systems," *IEEE Trans. Syst. Man Cybern. C, Appl. Rev.*, v. 37, n. 6, pp. 1067–1080, 2007.

[9] J. -H. Kim, K. S. Min, and W. -Y. Yeo, "A design of irregular grid map for large-scale Wi-Fi LAN fingerprint positioning systems," *Sci. World J*, v. 2014, Art. ID 203419, pp. 1–13, 2014.

[10] Y. Han, H. Ma, and L. Zhang, "An efficient RF fingerprint positioning algorithm based on uneven grid layout," In *Proc. ICWMMN*, Beijing, 2015, pp. 250–254.

[11] D. W. Aha, D. Kibler, M. K. Albert, "Instance-based learning algorithms," *Machine Learning*, v. 6, pp. 37–66, 1991.

[12] P. Brida, J. Machaj, and J. Benikovsky, "A modular localization system as a positioning service for road transport," *Sensors (Basel)*, v. 11, n. 14, pp. 20274–20296, 2014.

[13] Q. Wang, Y. Feng, X. Zhang, Y. Sun and X. Lu, "IWKNN: An effective Bluetooth positioning method based on isomap and WKNN," *Mobile Info. Systems*, v. 2016, Art. ID 8765874, pp. 1–11, 2016.

[14] OpenStreetMap Project. Available at: www.openstreetmap.org. Access: 10 Aug 2017.

[15] M. Vuckovic et. al., "Space grid resolution impact on accuracy of the indoor localization fingerprinting," In *Proc. TELFOR*, Belgrade, 2011, pp. 321–324.

[16] L. Klozar and P. Jan, "Wireless network localization: optimization processing," In *Proc. ICDT*, Chamonix, 2012, pp. 45–49.

[17] M. Kuhn and K. Johnson, Applied Predictive Modeling. Springer: New York, 2013.